JTTEE5 14:524-529
DOI: 10.1361/105996305X76568
1059-9630/$19.00 © ASM International

Peer Reviewed

Evidence of Mechanical Interlocking of NiCr Particles Thermally Sprayed onto Al Substrates

W.J. Trompetter, M. Hyland, P. Munroe, and A. Markwitz

(Submitted November 21, 2004; in revised form March 23, 2005)

Ni-chrome alloy particles were thermally sprayed onto aluminum substrates using the high-velocity air fuel technique. The particle substrate interface was investigated with focused ion beam microscopy, cross-sectional scanning electron microscopy, and cross-sectional transmission electron microscopy. No evidence of melting or chemical bonding was found in the samples. Instead, evidence of mechanical bonding was found that had been predicted by a previous theoretical study by Grujicic et al. At locations where the particle and substrate are in intimate contact, the interface exhibited interlocking features. These features are caused by the effects of turbulence due to interfacial instability and mixing at the interface during the coating process, resulting in a strong particle-substrate bond. Conversely, separated interfaces exhibited smooth surfaces, suggesting insignificant bonding between the particle and the substrate. The discovery of these interfacial formations, together with no evidence of chemical bonding across the particle-substrate interface indicate that mechanical interlocking is the dominant bonding mechanism.

Keywords adhesion of TS coatings, coating, influence of properties, substrate interaction

1. Introduction

Chemical bonding and mechanical interlocking are the two main bonding mechanisms that have been proposed for thermal spray coatings (Ref 1-4). Evidence of chemical bonding has been found in thermal spray coatings in which the feedstock material becomes molten or semimolten during the coating process. For example, such bonding has been identified in coatings prepared using plasma spraying (Ref 4-6), flame wire processing (Ref 7), and high-velocity oxyfuel (HVOF) spraying (Ref 8). However, it remains unclear which bonding mechanisms are dominant when the feedstock remains unmolten during the coating process (Ref 1-4).

In this study, Ni-chrome alloy particles were thermally sprayed onto aluminum substrates using the high velocity air fuel (HVAF) technique. The HVAF thermal spray technique uses kerosene and compressed air for combustion to accelerate a powder feedstock onto a substrate. The HVAF system was originally developed as a cheaper alternative to the HVOF thermal spray process. Initial studies suggest that coatings sprayed with HVAF have the advantage of not exhibiting the oxidation or decarburization effects observed in HVOF coatings (Ref 9-11). The HVAF technique is a low-temperature thermal spray process compared with HVOF; their typical combustion temperatures have been estimated (Ref 12) to be 1870 and 2650 °C, respectively. The gas cools as it leaves the combustion chamber and expands into the nozzle where the gas jet achieves supersonic expansion. Hence, the gas temperature in the nozzle where the feedstock powder is inserted is much lower than the gas temperature in the combustion chamber. For a chamber pressure of 414 kPa (60 psi), the gas temperature falls to approximately 1300 °C in the diverging section of the nozzle (Ref 12), which is below the melting point of NiCr powder (melting point 1400 °C). In addition, the contact time of the spray particles with the gas jet is quite short (i.e., on the order of 200 μs for a particle velocity of 700 m/s and a spray distance of 15 cm), and the particles will become only partially heated. As the spray particles and gas travel from the gun to the substrate, the gas continues to cool as it expands, resulting in particles with high kinetic energy, but with low thermal energies.

The temperature of the substrate during the thermal spray process depends not only on the temperature of the impacting powder particles, but also on how much of the powder particle kinetic energy is converted into thermal energy, as well as on the additional heating associated with the gas jet. In this article, the interface between the Ni-chrome particles and the aluminum substrate (melting point 660 °C) has been investigated to determine whether interfacial melting has occurred and which bonding mechanisms are present.

2. Experimental

The commercial Ni-chrome alloy powder (Ni80/Cr20, 5-45 μm) supplied by Sulzer Metco was thermally sprayed onto polished aluminum substrates using an HVAF thermal spraying technique (Ref 12). The gun was operated with a chamber pressure of 324 kPa (47 psi), and the gun-substrate spray distance was 15 cm. The individual splat samples shown in Fig. 1 were

W.J. Trompetter and **A. Markwitz,** Institute of Geological and Nuclear Sciences, P.O. Box 31312, Lower Hutt, New Zealand; **M. Hyland,** Department of Chemical and Materials Engineering, University of Auckland, Auckland, New Zealand; and **P. Munroe,** Material Science and Engineering, University of New South Wales, Sydney NSW 2052, Australia. Contact e-mail: B.Trompetter@gns.cri.nz.

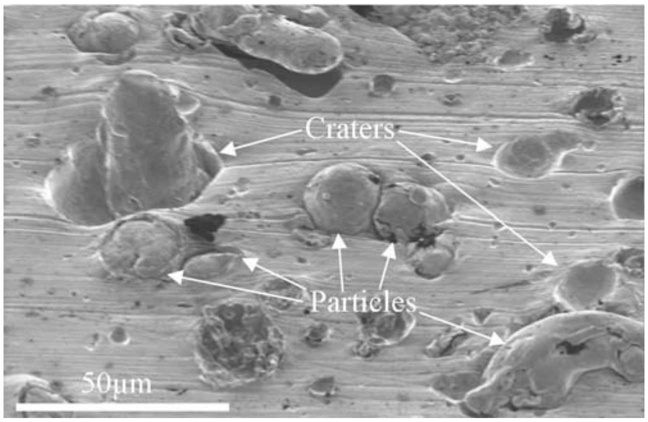

Fig. 1 An FIB secondary electron image of the aluminum substrate sample with a low density of sprayed NiCr particles

achieved by passing the HVAF gun across the substrate at speeds of 2 to 20 cm/s. It should be noted that passing the jet over the substrate to produce the single-splat particles has the advantage of lowering the exposure of the sample to the jet. A slower passing speed or repeated passing of the jet over the sample would allow the temperature to build within the sample. Hence, higher temperature effects may be possible in more densely coated samples.

The samples were investigated with an optical microscope, a focused ion beam (FIB), cross-sectional scanning electron microscopy (SEM), and cross-sectional transmission electron microscopy (TEM). The FEI xP200 (FEI, Portland, OR) FIB miller (Ref 13, 14) uses a focused beam of 30 keV gallium ions to scan over the surface of a specimen. The gallium beam at low currents (10-70 pA) can be used to produce high-resolution images of the sample via secondary electrons emitted during ion beam specimen interactions; alternatively, at high currents (1000-7000 pA) the beam can be used to rapidly sputter away the specimen. The highly focused scanning gallium beam allows the very rapid preparation of high-quality TEM cross sections to be milled. Other TEM polishing and sectioning methods such as ultramicrotomy or tripod polishing were found to alter and distort the samples, whereas the FIB milling process imparts very little stress on the sample. The FIB has the added advantage that it can mill at any location and from any orientation within a sample. Hence, the FIB provides the user with the capability to produce very thin (i.e., ~100 nm) sections at almost any desired location in a sample that is suitable for TEM examination.

Very good-resolution images by TEM were obtained using a Philips CM200 (Amsterdam, The Netherlands) with a 200 keV field emission gun equipped with an energy-dispersive x-ray system for elemental analysis. The SEM examinations were carried out using a Phillips XL30S with a 20 keV electron beam and a through-the-lens detector.

3. Results and Discussion

Figure 1 shows individual NiCr particles embedded in an aluminum substrate viewed using a FIB. Craters are additionally observed where the particles have bounced off the surface. There are more bonded particles than craters, indicating that efficient coating has been achieved. The particles that have bonded to the surface have a range of diameters (5-40 μm) and are mostly smooth, round particles with similar morphology to the original powder, indicating that they have remained solid during the coating process. The crater surfaces appear generally smooth without any evidence of surface roughness or turbulence effects that could occur during an impact.

Polished sectioned samples viewed with a scanning electron microscope show that individual particles deform but stay intact as they are embedded into the substrate (Fig. 2), indicating that they remain below the melting temperature during impact. This is consistent with nuclear reaction analysis measurements (Ref 15, 16) showing that the oxide content of the HVAF-sprayed NiCr coating is not significantly greater than the oxide content of the starting powder, which is indirect evidence that the particle temperature is very low. Similar observations are found in the cold spray process where similar features of the coating particles are observed and the oxide content of the particles also remains constant during the coating process (Ref 3, 17, 18). Conversely, HVOF- or plasma-sprayed particles become fully molten or semimolten during the coating process forming splats that exhibit splash-type features in the coatings with increased oxide contents (Ref 9-11). Hence, the nature of the HVAF deposition process is closer to that seen in the cold spray process rather than HVOF or plasma spray processes.

A range of features is observed at the interfaces of the HVAF-sprayed Ni-chrome particles shown in Fig. 2. The three sections chosen show different degrees of turbulence at the particle-substrate interfaces. The term *turbulence* refers to the mixing of particle and substrate material at the interface to produce interlocking features such as vortices or interfacial roll-ups due to interfacial instability during an impact. Although the polishing process could have introduced some of the discontinuities observed at the interfaces, it is generally observed that closer contact occurs at locations with turbulent effects at the interfaces, whereas the interfaces are often separated at locations with smooth surfaces. This indicates that strong bonding occurs at locations with turbulent effects at the interface. In addition, the mixing or turbulent features are more prominent as the particle size increases.

Focused ion beam milling has been found to be an ideal technique for investigating interfaces that are buried several microns under the sample surface in greater detail. Figure 3 shows cross sections of embedded particles that were prepared by excavating a selected area of spray-coated samples. The excavated areas were selected to bisect the particle as shown in the inset images. The result is a high-quality cross section of the embedded particle in the substrate. A region of the particle-substrate interface is displayed in the larger images. Turbulent features at the interface between the Ni-chrome particles and the aluminum substrates are highlighted in the larger images. The turbulent interfacial features of the three different sized particles in Fig. 3 are observed to be more prominent as the particle size increases. This was also observed earlier in the polished cross sections viewed by SEM in Fig. 2 and is consistent with the amount of interfacial instability estimated by Reynolds number calculations (Ref 1). Because the Reynolds number is proportional to the particle diameter, the amount of interfacial instability that produces the turbulent features is also proportional to the par-

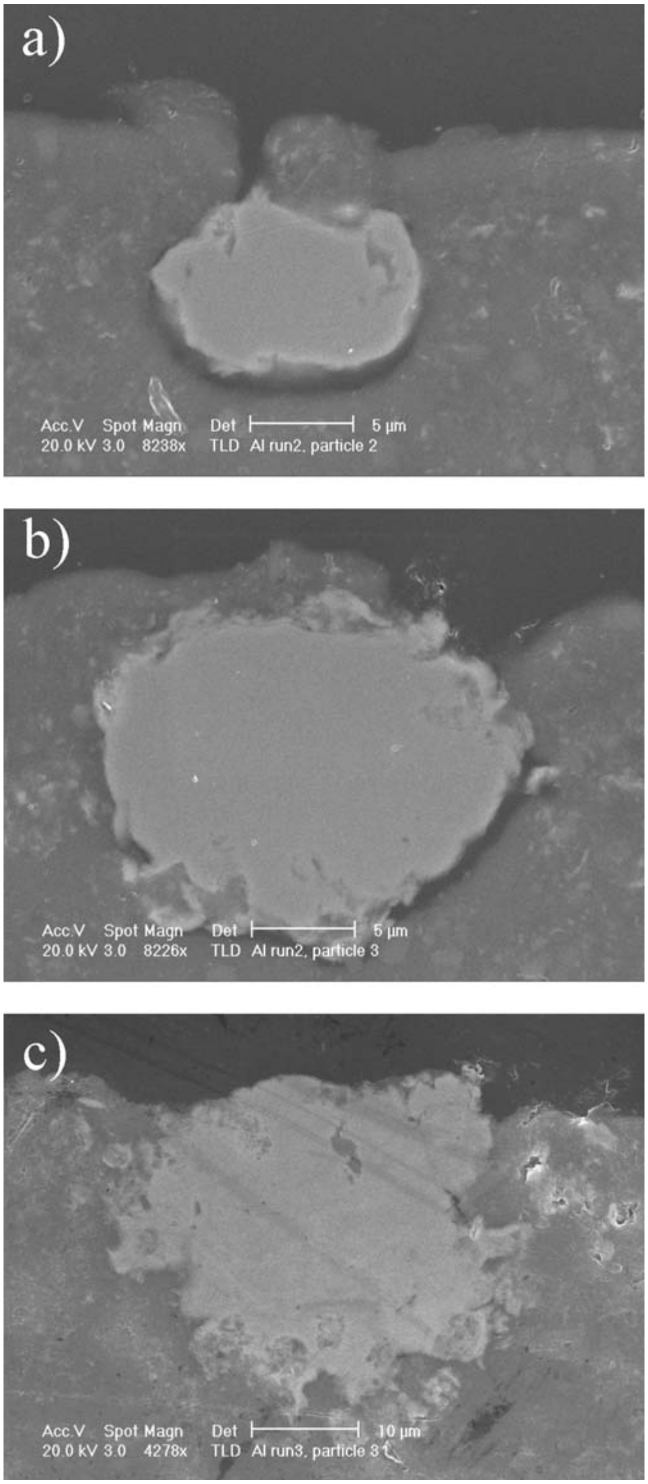

Fig. 2 Cross-sectional SEM images of individual NiCr particles embedded in an Al substrate with varying degrees of interfacial contact and interfacial turbulence: (a) low level of interfacial turbulence; (b) medium level of interfacial turbulence; and (c) high level of interfacial turbulence. The particle diameters are (a) 14 µm, (b) 21 µm, and (c) 36 µm.

ticle diameter. This is consistent with the observation that the size of the turbulent features observed in this study is proportional to the particle diameter.

The TEM image of the NiCr splat particle embedded in the aluminum substrate shown in Fig. 4 was also prepared using the FIB milling (Ref 13, 14). Figure 4 additionally indicates the location at the particle-substrate interface of the higher-magnification image and elemental maps displayed in Fig. 5. It can be seen that the Ni-chrome particle and the aluminum substrate are still joined together in this location, whereas at other locations along the interface separation has occurred. The main feature of the interface is an interlocking "jet" of aluminum extending approximately 100 nm into the NiCr particle.

To determine whether there are significant contributions of atomic diffusion or surface adhesion occurring between the particle and the substrate, the interface region was investigated for evidence of melting or recrystallization. A number of TEM images were taken from the interfacial regions of several particles (e.g., Fig. 4 and 5), which show no evidence of alteration within the Ni-chrome particle and the aluminum substrate, indicating that no melting or recrystallization has occurred during the spray-coating process. The TEM diffraction patterns of the aluminum substrate and the Ni-chrome particle adjacent to the interface (examples are shown as inserts in Fig. 5a) revealed high-angle crystal boundaries across the splat and the substrate interface, indicating an absence of chemical bonding. In addition, there were no measurable amounts of diffusion across the particle-substrate interface. Estimates of atomic diffusion extending less than 1 nm in typical cold-spraying conditions (Ref 1) suggest that diffusion would not be a dominant bonding mechanism under these conditions. Hence, the lack of evidence for interfacial chemical bonding and the observation of the interfacial turbulence indicate that mechanical bonding is the dominant bonding mechanism for NiCr particles that have been thermally sprayed onto aluminum with HVAF.

For bonding to occur in thermal spray coatings, it is has been observed that plastic flow and deformation occur in both the spray material and the substrate material (Ref 1-3, 19-21). In particular, the materials must be ductile or cosprayed with a ductile material to allow plastic deformation to occur. Additionally, the average particle velocity should exceed a minimum (material-dependent) critical velocity, which suggests that the kinetic energy must be sufficient to plastically deform the solid material and/or disrupt the surface oxide film. The particle kinetic energy at impact is typically significantly lower than the energies required for the particle to melt (Ref 1). The formation of the "surface-scrubbing" jets and high contact pressures are generally considered as prerequisites for good particle-substrate bonding.

Jets were first discovered in the very similar explosive welding process (Ref 20-25). However, these factors, while critical for attaining clean particle and substrate surfaces and an intimate contact between them, are not bonding structures. However, the formation of the jets indicates that plastic flow is occurring at the interface during the coating process. In certain conditions during plastic flow, it has been predicted (Ref 1) that interfacial instability can lead to the formation of interfacial roll-ups and vortices leading to high-strength interfacial bonding.

Grujicic et al. (Ref 1) and Yih (Ref 26) have demonstrated that an interfacial instability based on viscosity differences between the two flowing streams can grow during a collision event to produce significant turbulence at the interface even for vanishing Reynolds numbers. Grujicic et al. (Ref 1) proposed that bonding can occur through the interfacial instability-based

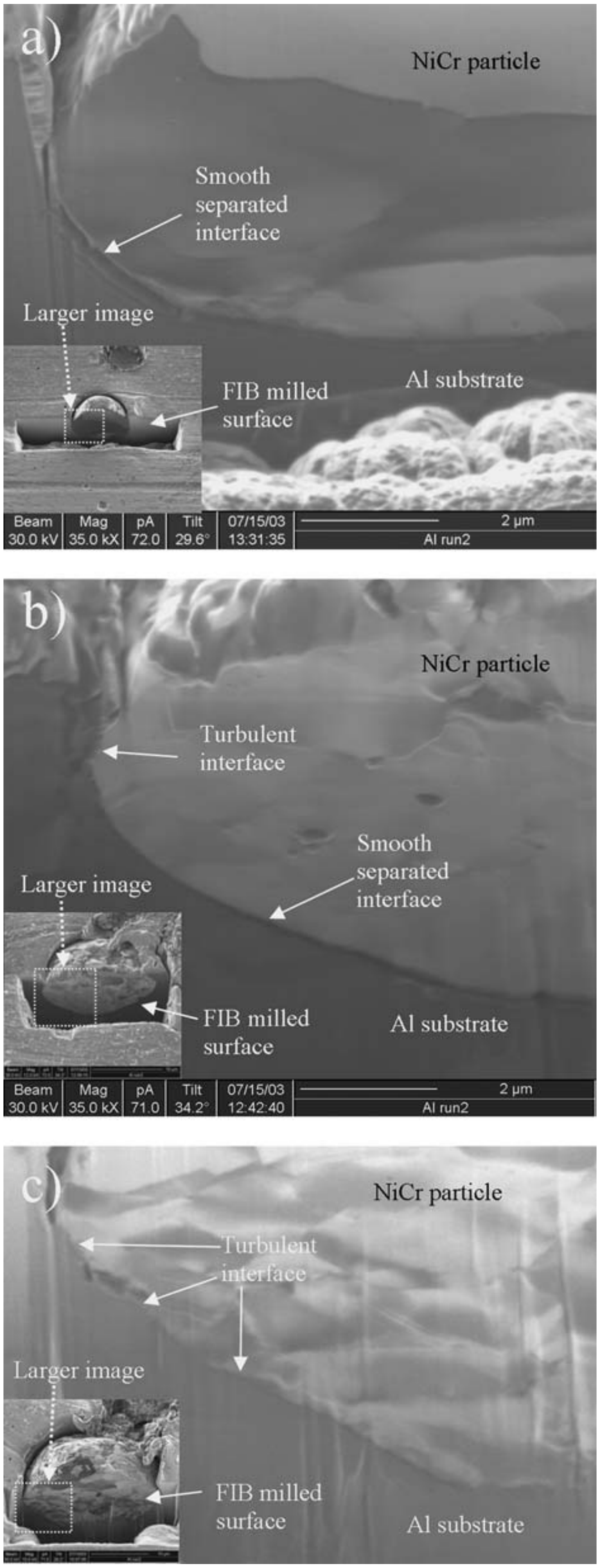

Fig. 3 Secondary electron images of three different NiCr particles embedded in Al substrates, sectioned and imaged with an FIB. The larger images show a region of the interface between the NiCr particle and the Al substrate. The inset images at the bottom left of each image show the whole sectioned surface and the location of the larger image. The particle diameters are (a) 11 µm, (b) 17 µm, and (c) 24 µm.

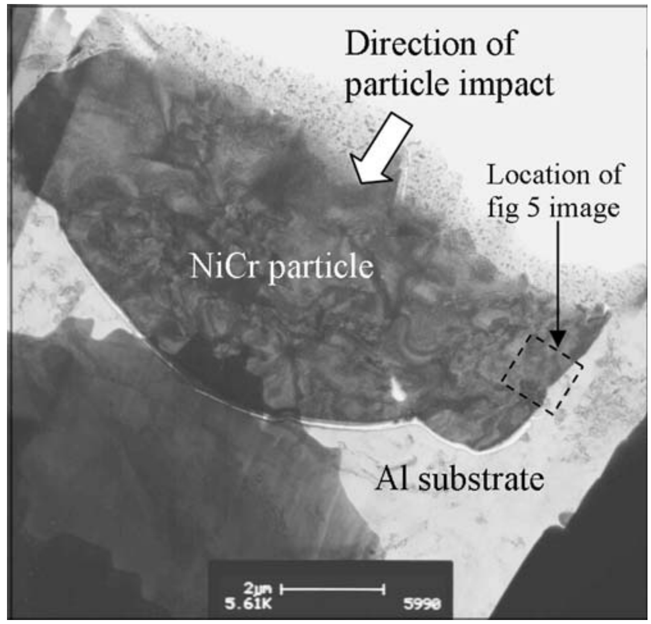

Fig. 4 Bright-field TEM image of an NiCr splat particle embedded in an aluminum substrate. The location of the higher-magnification image and elemental maps shown in Fig. 5 is additionally indicated. The particle diameter is approximately 12 µm.

mechanisms, which can lead to nano- and/or microlength-scale mechanical material mixing/interlocking mechanisms at an interface.

The dense NiCr particles sprayed onto soft aluminum substrates have proven to be good candidates for investigating turbulent effects due to the large difference in density (and kinematic viscosity) between Al (2.7 g/cm^3) and NiCr (8.4 g/cm^3). In this study, the interfacial turbulence between NiCr particles and aluminum substrates has been observed to range in size from 100 to 1000 nm. The turbulent behavior was observed to coincide with stronger bonding at locations where the interface was well-bonded, whereas the interface has separated at places where the surfaces are smooth. The interfacial formations at well-bonded interfaces suggest that mechanical interlocking is the dominant bonding mechanism.

4. Conclusions

The interface between the Ni-chrome particles and the aluminum substrates has been investigated with FIB, cross-sectional SEM, and cross-sectional TEM. Interlocking features were found at certain locations along the particle-substrate interfaces. Vortices of aluminum were found to extend 100 to 1000 nm from the substrate into thermally sprayed NiCr particles. The size of the turbulent features was proportional to the particle diameter, which is in agreement with the amount of interfacial instability estimated by Reynolds number calculations.

For mixing or turbulent behavior to occur, the spray-coating material needs to be able to “flow.” This fits well with the experimentally observed prerequisites for producing good-quality coatings by spraying with a minimum threshold of kinetic en-

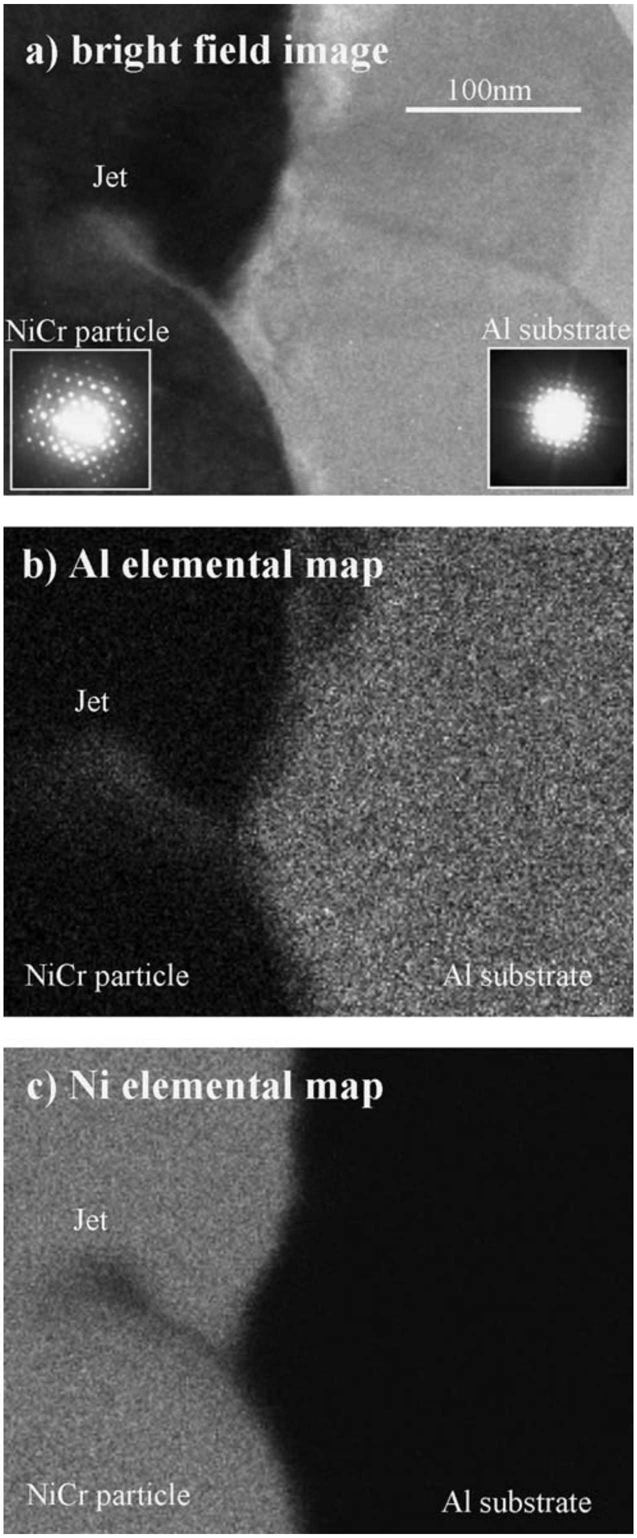

Fig. 5 An SEM image of the particle and substrate interface: (a) bright-field image with diffraction pattern inserts of the NiCr particle and the Al substrate, (b) Al elemental map, and (c) Ni elemental map

ergy and having to use ductile materials. The ductile materials mean that they are capable of flow, and the minimum threshold energy means that a certain flow is required before turbulent behavior and bonding is achieved. This type of bonding was predicted recently by Grujicic et al. (Ref 1).

In cross-sectional images of individual particles, it was observed that strong bonding occurred at the interface where there was turbulent behavior, whereas the interface has separated at places where the surfaces are smoother. In addition, TEM investigations revealed high-angle crystal boundaries across the splat and the substrate interface, indicating that no significant chemical bonding was occurring across the interface. The observation of interfacial formations together with no evidence of chemical bonding across the interface suggest that mechanical interlocking is the dominant bonding mechanism for Ni-chrome alloy particles that have been thermally sprayed onto aluminum substrates using the HVAF technique.

Acknowledgment

This work was performed under a research contract with the New Zealand Foundation for Research, Science and Technology (C05X0008).

References

1. M. Grujicic, J.R. Saylor, D.E. Beasley, W.S. DeRosset, and D. Helfritch, Computational Analysis of the Interfacial Bonding Between Feed-Powder Particles and the Substrate in the Cold-Gas Dynamic-Spray Process, *Appl. Surf. Sci.,* Vol 219, 2003, p 211-227
2. R.C. Dykhuizen, M.F. Smith, D.L. Gilmore, R.A. Neiser, X. Jiang, and S. Sampath, Impact of High Velocity Cold Spray Particles, *J. Therm. Spray Technol.,* Vol 8 (No. 4), 1999, p 559-564
3. T.H. Van Steenkiste, J.R. Smith, R.E. Teets, J.J. Moleski, D.W. Gorkiewicz, R.P. Tison, D.R. Marantz, K.A. Kowalsky, W.L. Riggs II, P.H. Zajchowski, B. Pilsner, R.C. McCune, and K.J. Barnett, Kinetic Spray Coatings, *Surf. Coat. Technol.,* Vol 111, 1999, p 62-71
4. S. Dallaire, Influence of Temperature on the Bonding Mechanism of Plasma-Sprayed Coatings, *Thin Solid Films,* Vol 95, 1982, p 237-244
5. H.-D. Steffens, B. Wielage, and J. Drozak, Interface Phenomena and Bonding Mechanism of Thermally-Sprayed Metal and Ceramic Composites, *Surf. Coat. Technol.,* Vol 45, 1991, p 290-308
6. S. Kitahara and A. Hasui, A Study of the Bonding Mechanism of Sprayed Coatings, *J. Vacuum Sci. Technol.,* Vol 11, 1974, p 747-753
7. R. McPherson, The Relationship Between the Mechanism of Formation, Microstructure and Properties of Plasma-Sprayed Coatings, *Thin Solid Films,* Vol 83, 1981, p 297-310
8. H. Li, K. A. Khor, and P. Cheang, Impact Formation and Microstructure Characterization of Thermal Sprayed Hydroxyapatite/Titania Composite Coatings, *Biomaterials,* Vol 24 (No. 6), 2003, p 949-957
9. L. Jacobs, M.M. Hyland, and M. De Bonte, Comparative Study of WC-Cermet Coatings Sprayed Via the HVOF and HVAF Processes, *J. Therm. Spray Technol.,* Vol 7, 1998, p 213-218
10. A.M. Ahmed, R.H. Rangel, V.V. Sobolev, and J.M. Guilemany, In-Flight Oxidation of Composite Powder Particles During Thermal Spraying, *Int. J. Heat Mass Transfer,* Vol 44 (No. 24), 2001, p 4667-4677
11. S.V. Joshi and R. Sivakumar, Particle Behaviour During High Velocity Oxy-Fuel Spraying, *Surf. Coat. Technol.,* Vol 50 (No. 1), 1991, p 67-74
12. J.A. Browning, Hypervelocity Impact Fusion: A Technical Note, *J. Therm. Spray Technol.,* Vol 1 (No. 4), 1992, p 289-292
13. N. Rowlands and P. Munroe, FIB for the Evaluation of Non-Semiconductor Materials, *Microstruct. Sci.,* Vol 26, 1998, p 233-242
14. J.M. Cairney, R.D. Smith, and P.R. Munroe, Transmission Electron Microscope Specimen Preparation of Metal Matrix Composites Using the Focused Ion Beam Miller, *Microsc. Microanal.,* Vol 5, 2000, p 452-462
15. W.J. Trompetter, A. Markwitz, and M. Hyland, Use of IBA Techniques to Characterize High Velocity Spray Coatings, *Modern Phys. Lett.,* Vol B15, 2002, p 1428-1436

16. W.J. Trompetter, A. Markwitz, and M. Hyland, Role of Oxides in High Velocity Thermal Spray Coatings, *Nucl. Instrum. Methods,* Vol B190, 2002, p 518-523
17. A.O. Tokarev, Structure of Aluminium Powder Coatings Prepared by Cold Gas Dynamic Spraying, *Met. Sci. Heat Treat.,* Vol 35, 1996, p 136-139
18. C. Rinaldi, L. Ferravante, F. Uberti Paci, and P. Bianchi, Extensive Characterization of Dense and Corrosion Resistant Coatings Produced by Improved Shrouded Techniques, Thermal Spray 2001: New Surfaces for a New Millenium, C.C. Berndt, K.A. Khor, and E.F. Lugscheider, Ed., May 28-30, 2001 (Singapore), ASM International, 2001, p 1185-1193
19. C. Borchers, F. Gärtner, T. Stoltenhoff, H. Assadi, and H. Kreye, Microstructural and Macroscopic Properties of Cold Sprayed Copper Coatings, *J. Appl. Phys.,* Vol 93, 2003, p 10064-10070
20. H. Assadi, F. Gärtner, T. Stoltenhoff, and H. Kreye, Bonding Mechanism in Cold Gas Spraying, *Acta Mater.,* Vol 51, 2003, p 4379-4394
21. M.A. Meyers, N.N. Thadhani, and L.H. Yu, Explosive Shock Wave Consolidation of Metal and Ceramic Powder, *Shock Waves for Industrial Applications,* L.E. Murr, Ed., William Andrew/Publishing/Noyes, NJ, 1988, p 265-334
22. A.A. Deribas and I.D. Zakharenko, Surface Effects with Oblique Collisions Between Metallic Plates, *Fiz. Gor. Vzr.,* Vol 10, 1974, p 409-421
23. M. Hammerschmidt and H. Kreye, Microstructure and Bonding Mechanism in Explosive Welding, *Shock Waves and High Strain-Rate Phenomena in Metals,* M.A. Meyers and L.E. Murr, Ed., Plenum Press, New York, 1981, p 961-973
24. R. Prümmer, *Explosivverdichtung pulvriger Substanzen: Grundlagen, Verfahren, Ergebnisse,* Springer, Berlin, 1987 (in German)
25. D. Raybould, Properties of Stainless Steel Compacted Dynamically to Produce Cold Interparticle Welding, *J. Mater. Sci.,* Vol 16, 1981, p 589-598
26. C.S. Yih, Instability Due to Viscosity Stratification, *J. Fluid Mech.,* Vol 27, 1967, p 337-352